J Mater Sci (2007) 42:8529–8536
DOI 10.1007/s10853-007-1740-5

A recording microindentation instrument for in situ study of crack initiation in glass

Trevor E. Wilantewicz · James R. Varner

Received: 19 February 2007 / Accepted: 2 April 2007 / Published online: 23 June 2007

Abstract A recording microindentation instrument equipped with optical observation and acoustic emission detection was built and used to examine, in situ, the crack initiation behavior of a commercial soda-lime-silica based float glass from contact with a Vickers diamond indenter. Indenter motion was provided by a piezoelectric actuator, while a strain gage load cell and capacitance displacement gages simultaneously monitored the indenter load and displacement, respectively, on the glass. It was found that both the maximum load and total indenter contact time influence the initiation behavior. Crack initiation occurred more readily when the total contact time and maximum load were increased. Increasing the maximum load from 0.2 kgf to 4 kgf resulted in the initiation of median-radial cracks on unloading at 6% Fmax up to 50% Fmax, respectively. In contrast, the initiation of lateral cracks was not significantly affected by the total contact time or the maximum load. Examination of the indentation cross-sections beneath 1 and 4 kgf indentation sites revealed well-developed median-radial and lateral crack systems.

Introduction

Recording microindentation testing has been used by many to study the indentation response of a variety of materials [1–7]. In this testing format the load and displacement of an indenter are simultaneously and continuously monitored throughout the entire indentation cycle as the indenter is pushed in and then withdrawn from the sample [1]. The technique can allow the in situ determination of the threshold load for cracking in a variety of materials [4, 7–9]. In addition, for materials undergoing elastic–plastic deformation, this testing format allows quantifying this by direct measurement of the elastic recovery of the specimen in the vertical (depth) direction on unloading of the indenter [1, 3]. This testing format also enables the determination of hardness numbers that are load-independent [5], and the energy consumed by permanent deformation [2]. Young's modulus of a material may also be estimated by proper analysis of the unloading portion of the curve [2, 6, 10]. This may be useful for thin film materials, for example, where more conventional techniques cannot be used.

More pertinent to the current work is the use of the technique to monitor the crack initiation behavior of brittle materials in situ with respect to the loading and unloading indentation cycles. Several studies have looked at this in the past, including those by Cook and Pharr [4] Wagner [7], Lawn et al. [8] and Canfield [9]. In these studies a Vickers indenter was pushed into the specimen at a controlled, slow rate, allowing the load to build-up gradually, and at the same time visual observation of the contact site under high magnification enabled the determination of crack threshold loads. Wagner [7] and Canfield [9] also utilized acoustic emission detection to help identify the onset of cracking. In addition to studying different glass compositions, Cook and Pharr [4] examined some crystalline ceramic materials as well, and Wagner [7] examined other important glass systems in addition to soda-lime-silica, including borosilicate and aluminosilicate glasses.

T. E. Wilantewicz (✉) · J. R. Varner
Impact Physics Branch, US Army Research Laboratory (ARL), ATTN: AMSRD-ARL-WM-TD, Aberdeen Proving Ground, MD 21005, USA
e-mail: twilantewicz@comcast.net;
trevor.wilantewicz@arl.army.mil

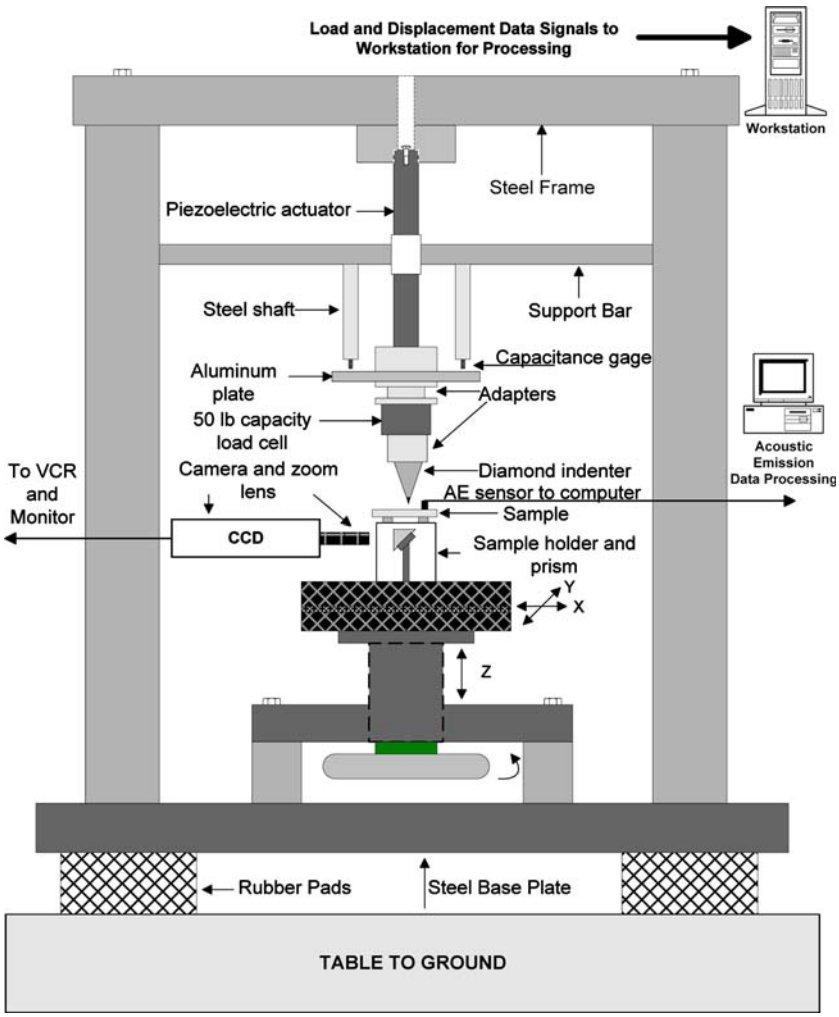

Fig. 1 Schematic diagram of the recording microindenter instrument. The system was approximately 18 inches tall and 15 inches wide

The current paper describes the operation of a newly constructed recording microindentation instrument for in situ monitoring of the crack initiation behavior of materials, and presents some results for tests on a commercial soda-lime-silica based float glass.

Experimental procedures

The recording microindenter

A recording microindenter was built so that crack initiation using relatively high indentation loads, up to 4 kgf, could be investigated in situ. A schematic of the system is shown in Fig. 1. The whole assembly rested on a sturdy table, and four rubber pads were positioned between the steel base plate of the instrument and the table in order to dampen any vibrations. The operation of the instrument was computer controlled. The soft-PZT piezoelectric actuator[1] pushes the Vickers diamond into the glass sample while the load and displacement of the diamond are simultaneously monitored, as a function of time, by the strain-gauge load cell[2] and two capacitance displacement gauges,[3] respectively. The load cell had a 22.7 kgf capacity, and the displacement gauges had a maximum measuring range of 500 μm. Before passing to the workstation computer, the signals from both the load cell and capacitance gauges passed through their respective signal conditioners and amplifiers. When combined with the 16-bit digital-to-analog (D/A) card[4] in the computer, the theoretical load and displacement resolutions were 0.35 g and 7.6 nm, respectively. For driving the piezoelectric actuator, the D/A card was capable of a 12-bit digital-to-analog conversion, which when combined with the 60 μm total displacement capability of the actuator, resulted in a displacement resolution of approximately

[1] Model PZL-60, Burleigh Instruments, Inc., Fishers, New York.

[2] Lebow Model 3189-50, Eaton Corp. Lebow Products, Troy, Michigan.

[3] Model HPT-40, Capacitec Corporation, Ayer, Massachusetts.

[4] Model AT-MIO-16XE-50, National Instruments Corp., Texas.

14 nm. The displacement rate was the same on loading and unloading. A program was written using LabView software which allowed total user control over the maximum load, displacement rate, and hold time desired. The data that were collected from a test run were the time, load, and displacement readings from both capacitance gauges. The averaged readings from both displacement gauges was used to calculate a single displacement point for each load value. A threshold load of 1.5 g was used before data were collected in order to prevent false triggering of data collection. This was necessary because of the small amount of electrical noise in the system.

Optical system

A zoom lens was fitted to a CCD camera, which was connected to a 13″ television, and allowed in situ optical observation of the indentation crack initiation process from below the specimen. A VCR was also set-up to record the entire indentation process observed on the monitor. Fiber-optic lamps illuminated the indentation site. A glass prism directed the light, by total internal reflection, through a 90° angle into the zoom lens and CCD camera. The transparent sample sits on a ball bearing race (sample holder), which is hollow in the center to allow light to pass through to the prism. By adjusting the zoom lens, the magnification of an image on the monitor could be varied from about 100× to 740×. For most of the crack initiation experiments the magnification was kept at 740×, permitting a detailed observation of the crack initiation process.

Acoustic emission system

A PAC MISTRAS-2001 acoustic emission (AE) system[5] was used to detect the acoustic emissions resulting from the crack initiation tests, in situ. The system was fully computerized and capable of simultaneously collecting and processing classical AE features (counts, hits, duration, energy, rise-time, amplitude, frequency, etc.) and perform transient waveform recording as well, all in real-time. A broadband, resonant-type, single-crystal piezoelectric transducer from Physical Acoustics Corporation (PAC), called PICO, was used as the AE sensor. It measured 5 mm diameter and 4 mm tall. The sensor had a resonance frequency of 513.28 KHz, and an optimum operating range of 200–750 KHz. The sensor was connected to a 1220 A preamplifier from PAC, set to a 40 dB gain, which translated into a 100-fold pre-amplification of the signal. The threshold level and other settings of the acoustic emission system were adjusted to optimize the detection of crack initiation events.

[5] Physical Acoustics Corporation (PAC), Princeton, New Jersey.

Crack initiation testing

The float glass came in large sheet-form, about 3.2 mm thick, from which smaller rectangular pieces approximately 30 mm × 25 mm were cut. One piece was used for the crack initiation tests, another piece for mechanical properties testing, and another piece for density measurements. All crack initiation tests were carried out on the atmosphere side of the float glass, which was determined using an ultraviolet (UV) lamp, in which the tin-side fluoresces a purple color when exposed to UV light. The condition of the glass surfaces were flat and smooth such that no grinding or polishing were necessary. Specimens were, however, annealed at 564 °C for 1 h to remove any residual stress, then slow cooled at a set rate of 1 °C/min to room-temperature. The glass transition temperature of the float glass was determined to be 554 °C using a differential scanning calorimeter. The crack initiation tests were carried out in laboratory air where the temperature and humidity were about 24 °C and 20%, respectively. An air conditioning system was used to keep the relative humidity low. Just prior to testing, the specimen was ultrasonicated in reagent grade alcohol (90% ethanol, 5% methanol, 5% isopropanol) to remove any contamination. The piece of float glass, atmosphere side up, was placed on the sample holder, and the AE sensor was attached to the top surface, away from the center of the sample, using high-vacuum grease. Tests were conducted at maximum loads of 4, 2, 1, and 0.2 kgf with a 0.2 μm/s indenter displacement rate. There was no hold time at the maximum load, except for the 2 kgf tests, where the maximum load was held for 30 s before unloading. In addition, three additional sets of experiments were conducted, one using a 2 kgf maximum load and 1 μm/s indenter displacement rate with no hold time, another using 4 kgf maximum load and 0.2 μm/s rate with a 30 s hold time, and another using a 1 kgf maximum load with a 1.5 μm/s displacement rate with no hold time. At least 10 test runs were conducted at each load, except 5 tests were made at 0.2 kgf. Each test was conducted on a fresh area of the specimen by suitable translation of the x-y stage. Subsequent analysis of the AE, VHS video, and load-displacement data were used to determine the threshold loads for crack initiation for each test. The types of cracks which formed were determined by careful examination of the VHS video, and by post-test optical microscopy and sectioning of indentation sites.

Mechanical properties

Density was measured on a separate piece of glass using the Archimedes method with kerosene as the immersion medium. Hardness measurements using a Vickers diamond were made on another test specimen. Ten indentations were

made with a 200 gf load held for 15 s using a conventional hardness tester. The Meyers hardness (load/projected area) was calculated using Eq. 1

$$H = \frac{2P}{d^2} \quad (1)$$

where,

H = hardness (N/m^2)
P = load (N)
d = average indentation diagonal length (m)

Young's modulus was measured using the ultrasound pulse-echo technique. Indentation toughness was determined by measuring the surface lengths of cracks extending from indentations made at 1 kgf on a conventional hardness tester, then using Eq. 2 to calculate the toughness, after Anstis et al. [11]:

$$K_C = 0.016\left(\frac{E}{H}\right)^{1/2}\frac{P}{c^{3/2}} \quad (2)$$

where,

K_C = indentation toughness ($Pa\sqrt{m}$)
E = Young's Modulus (N/m^2)
H = hardness (N/m^2)
c = median-radial crack length from center of indentation to crack tip (m)

Twelve indentations were made, and immediately after each indentation the surface traces of the four major median-radial cracks were measured from the center of indentation to the crack tip. These four values were then averaged and a toughness value calculated for each indentation. The Meyers hardness was used for H in Eq. 2. The 12 toughness values were then averaged.

Results

Mechanical properties

Table 1 lists the mechanical properties of the float glass which were determined in this work. The values are typical of a commercial silicate flat glass, as the values for hardness, Young's modulus, and toughness agree fairly well with data from other researchers testing glasses of similar composition [4, 12, 13].

Table 1 Mechanical properties data

Hardness, H (GPa)	Young's Modulus, E (GPa)	Poisson's ratio, ν	Indentation toughness, Kc ($MPa\sqrt{m}$)	Density, ρ (g/cm^3)
5.7 ± 0.1	73.6 ± 1.4	0.22 ± 0.02	0.69 ± 0.02	2.52

Crack initiation tests

For all experiments, it was observed that median-radial cracks initiated in an unstable manner i.e., popped-in, on the unloading indentation half-cycle, that is, as the indenter was being withdrawn from the glass. However, the loads at which these cracks initiated varied with the maximum load used in the test and the total contact time. The initiation of all median-radial cracks took place all at once for the 4 kgf maximum load tests, but this was not true for the 0.2 and 1 kgf tests. For the 2 kgf tests, some tests had all cracks initiate at once, and others did not. For the 0.2 and 1 kgf tests, what appeared to be two separate median-radial cracks would first initiate at opposite indentation corners at the same time, this was then followed by the initiation of the additional median-radial cracks from the other two corners at separate instances in time (load) as unloading continued. Figure 2 plots the normalized initiation loads expressed as a percentage i.e., $(F_{init}/F_{max})*100$, as a function of the maximum load. It is seen that the normalized load at fracture decreases with decreasing maximum load, although rate effects are also apparent. The loads plotted correspond to the initiation of the first median-radial cracks observed. As the load is removed, the stresses build in the material until a critical stress is reached, at which point the cracks initiate. This is because as unloading of the indenter occurs, the elastic compressive stresses continually decrease, and are replaced by the tensile stress field of the

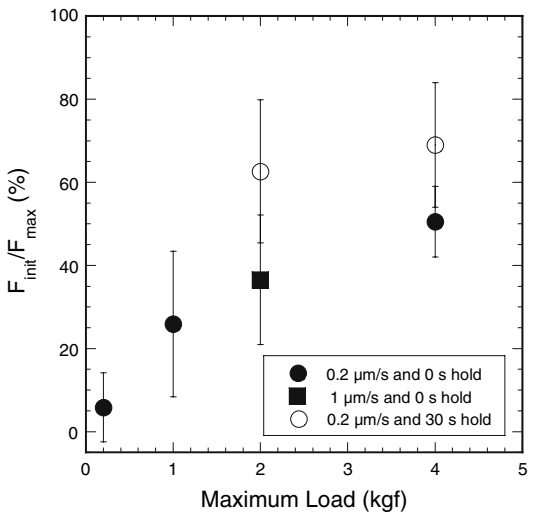

Fig. 2 The normalized initiation load (F_{init}/F_{max}), expressed as a percentage, for the first median-radial cracks to initiate in the float glass on the unloading half-cycle, as a function of the maximum set load. Additional contact parameters for the tests are also indicated. Error bars are ± one standard deviation

residual component. Thus, the net tensile stress at any fixed location increases until a critical stress level is reached. Therefore, lower normalized initiation loads are indicative of increased resistance to crack initiation. It is also evident that increasing the indenter displacement rate from 0.2 μm/s to 1.0 μm/s decreased the average normalized initiation load from 63 ± 17% to 37 ± 16% for the 2 kgf maximum load tests. In addition, for the 4 kgf tests, decreasing the hold time at the maximum load from 30 s to 0 s lowered the average normalized initiation loads from 69 ± 15% to 51 ± 8%, respectively. Thus, decreasing the hold time at the maximum load has qualitatively the same effect as increasing the indenter displacement rate. Near, or just after complete unloading of the indenter (<5% F_{max}), a system of lateral cracks were observed to initiate for all tests except those at 0.2 kgf. The normalized initiation loads for the lateral cracking were essentially independent of the maximum load and total contact time.

Figure 3 plots the normalized crack initiation time, which is the time at which the first median-radial cracks were observed to initiate, normalized to the total contact time i.e., t_{init}/t_{total}, as a function of the total contact time. All the data points have $t_{init}/t_{total} < 1$, indicating that cracks initiated during the unloading half cycle. There is an indication that as the total contact time increases, the normalized initiation time decreases i.e., cracks begin to initiate relatively sooner on the unloading cycle as the total contact time increases. However, the fact the trend is not very linear suggests that the maximum load also has an influence on the initiation behavior that is separate from any of the kinetic effects associated with the contact time. This point is discussed in more detail in the discussion section.

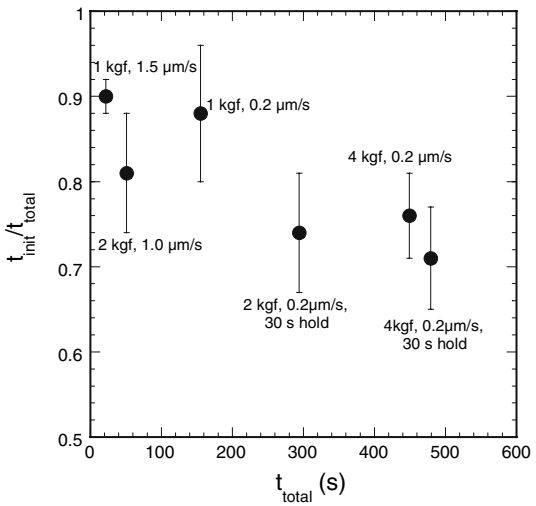

Fig. 3 The normalized initiation time as a function of the total contact time. The contact parameters associated with each of the data points are shown next to the points. Error bars are ± one standard deviation

Acoustic emission

Figure 4 plots the acoustic emission energy and count signals associated with the initiation of the first median-radial cracks. For the 0.2 kgf maximum load tests, no acoustic emission hits were detected, with the exception of a single hit for one of the tests; however, this produced a zero energy signal. The acoustic emission energy and count signals increase with load. Since more elastic strain energy is presumably stored in the glass as the maximum load increases, more of this energy should be available for release at the instant of crack initiation. The acoustic emission energy and count signal trends are consistent with this idea.

Post-test microscopy

Figure 5a and b shows representative indentation sites from the crack initiation tests in float glass at loads of 1 and 4 kgf, respectively. Well-developed median-radial cracks are apparent in both images, and extend outwards from near the four corners of the indentations. It is apparent that more than one initiation attempt took place around two of the corners of the 4 kgf indentation, where two additional major cracks around each of these corners can be seen. In comparison, for the 1 kgf indentation site, the additional initiation attempts which took place produced only very small cracks around two of the corners. Some of the 1 kgf indentation sites showed a pattern similar to the 4 kgf test sites i.e., more than one major median-radial initiation attempt at several of the corners, however this was rare. Figure 6a and b presents higher magnification images of the indentation sites in Fig. 5a and b, respectively, and clearly show shear faults parallel to the indentation sides.

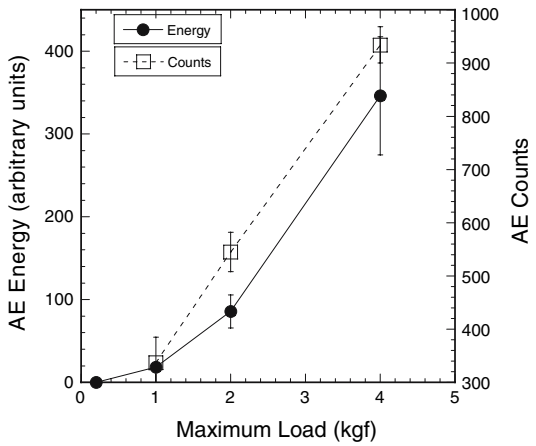

Fig. 4 Acoustic emission energy and count signals for the initiation of the first median-radial cracks in float glass as a function of the maximum load. Data for 2 kgf are for the 0.2 μm/s displacement rate and 30 s hold tests

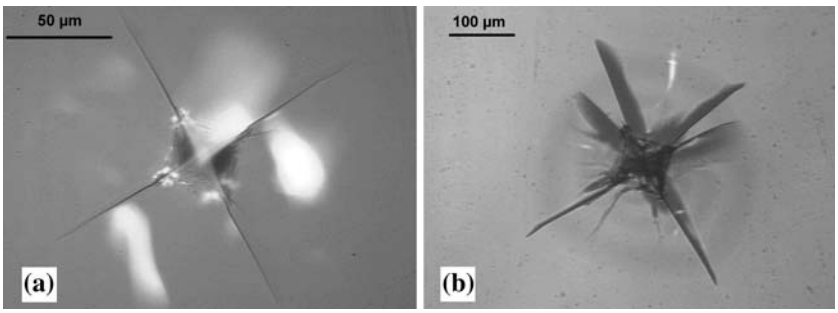

Fig. 5 Representative indentation sites in float glass from the crack initiation experiments. (**a**) 1 kgf. (**b**) 4 kgf. Reflected light optical microscopy with differential interference contrast conditions

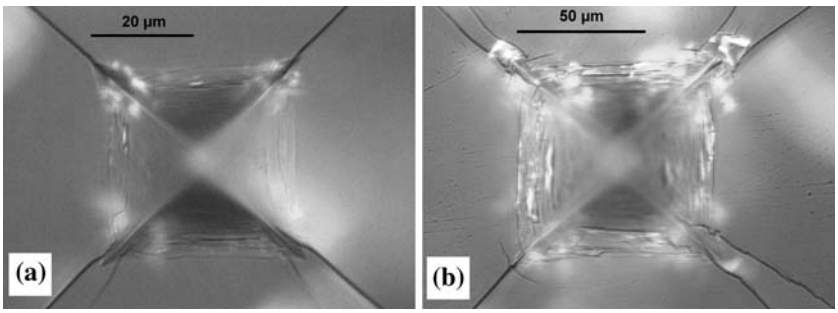

Fig. 6 (**a**) Higher magnification image of indentation site shown in Fig. 5(a). (**b**) Higher magnification image of indentation site shown in Fig. 5(b). Reflected light optical microscopy with differential interference contrast conditions. Note small partial ring cracks around several corners in (b)

Lawn et al. [8] have shown these faults to be the crack nuclei of median-radial cracks around Vickers indentations in soda-lime-silica glass. That is, stress concentration takes place along the faults, or at the intersection of faults, causing a median-radial crack to pop-in.

Cross-sections of 1 and 4 kgf indentation sites are shown in Fig. 7a and b, respectively. The arrest lines of two median-radial (MR) cracks in the plane of fracture are seen for both the 1 and 4 kgf indentation sites. Each of the two median-radial cracks appears to resemble a quarter-penny geometry, but when taken together form an essentially half-penny crack system. Sub-surface lateral cracks (LC) are seen to initiate from near the base of the damage zone (DZ) beneath the indentations. These features are only labeled in Fig. 7a.

Discussion

The current results show that the initiation behavior of median-radial cracks in float glass is sensitive to the maximum indentation load and total contact time. For a given maximum load, the indenter displacement rate will control the total contact time. Slower rates will cause the total contact time to increase compared to faster rates. On the other hand, for given displacement rate the maximum load achieved will control the total contact time, with higher maximum loads resulting in increased contact time. Although the maximum load used directly influences the total contact time, it is believed to also have an effect which is separate from the kinetic influences, as will be discussed below.

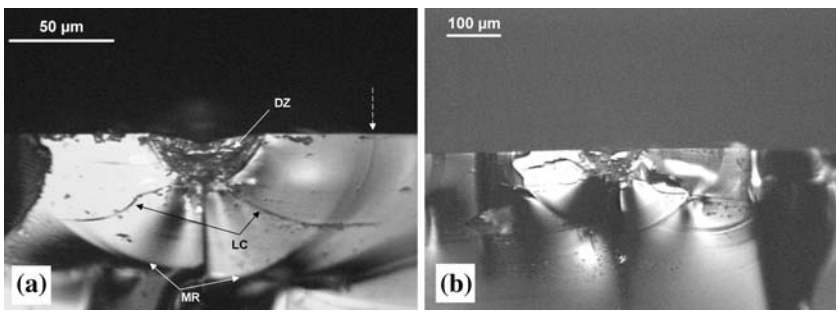

Fig. 7 Indentation cross-sections in float glass produced by sectioning indentations made with the recording microindenter on thin, ~1 mm thick, specimens. (**a**) 1 kgf; broken white arrow indicates, approximately, where median-radial crack ends on surface; see text for other descriptions. (**b**) 4 kgf. Reflected light optical microscopy with differential interference contrast conditions

The initiation results in Figs. 2 and 3 can be explained based on the effects of maximum load and total indenter contact time. First, the increased contact time associated with either (i) increasing the maximum load, (ii) decreasing the displacement rate, or (iii) increasing the hold time at the maximum load, is believed to result in an increased amount of slow crack growth of the incipient crack nuclei. This is believed to be due to stress corrosion of the crack nuclei caused by water vapor in the atmosphere, as previously found and discussed by Lawn et al. [8]. This would result in the incipient nuclei being in a more advanced stage of development earlier on the unloading half-cycle, resulting in quicker crack initiation i.e., at lower values of t_{init}/t_{total}. Second, increasing the maximum load increases the size of the shear faults. Figure 6 shows that the shear faults are longer, and possibly wider, for the 4 kgf indentation sites compared to the 1 kgf sites. Longer shear faults would provide crack nuclei in a more advanced stage of development than shorter faults, and hence cracks would be expected to initiate sooner e.g., at higher normalized loads or lower t_{init}/t_{total}. Lawn et al. [8], Dabbs et al. [14], and Hagan [15] have convincingly shown that shear faults, and/or the voids generated at the intersection of faults, serve as the nucleation sites for crack initiation around Vickers indentations in soda-lime-silica glass. If the data points in Fig. 3 were to have fallen perfectly on a straight line, then the total contact time could be deemed the only variable influencing the initiation results. The fact they do not lends further credence to the independent effect of the maximum load on the initiation behavior, as discussed above. It is also apparent in Fig. 2 that the rate of increase of F_{init}/F_{max} decreases as F_{max} increases. Cook and Pharr [4] found the initiation load to plateau at about 60% F_{max} for soda-lime-silica glass, beginning at a 20 N (~2 kgf) load. If, in the current work, tests were conducted at 2 kgf with a 0.2 μm/s rate and no hold time, this data point would be expected to fall somewhere between the two data points at 2 kgf shown in Fig. 2, since the total contact time would fall in between that for the two points shown. If this were the case, then a plateau would be observed, similar to that seen by Cook and Pharr [4]. A plateau would possibly indicate that some type of saturation in the indentation system was taking place. That is, one or more of the mechanisms associated with crack initiation, e.g., slow crack growth or the size of crack nuclei, stop changing, or are nullified by other new, unknown mechanisms. The initiation of all median-radial cracks at once for the 4 kgf tests, and for some of the 2 kgf tests, when compared to the 0.2 and 1 kgf tests where all cracks did not initiate at once (recall ''Crack initiation tests'' section), is consistent with more of the crack nuclei (shear faults) being in a more advanced stage of development for the higher load and higher contact time tests, thus enabling the Griffith criterion for fracture to be satisfied simultaneously for all crack nuclei. This assumes the cracks initiate when the stress at the flaw tip reaches some constant critical level, and which is particular for the material under consideration.

The relative independence of the lateral crack initiation loads with either the maximum load or the total contact time suggests that the lateral crack nuclei are less susceptible to stress corrosion, and hence rate effects do not show up in the initiation behavior. This may be due to the tendency for lateral cracks to initiate well below the surface, near the base of the damage zone, in which case diffusion of water to the lateral crack nuclei will be more difficult compared to crack nuclei near the surface.

The increase of acoustic emission energy with increased maximum load is consistent with increased elastic strain energy being stored in the glass, and hence released, at the higher maximum loads. This indicates there is more crack driving force, consistent with the observation that the length of the median-radial and lateral cracks around the indentations increased with the maximum load.

Summary

A recording microindentation apparatus was constructed and used successfully to study, in situ, the development of cracks around Vickers indentations in a commercial soda-lime-silica based float glass. The crack initiation behavior of the median-radial cracks was found to depend on the maximum load and the total contact time. The likely increase in the size of crack nuclei (shear faults) from slow crack growth due to stress corrosion from atmospheric water vapor with increasing total contact time, and the increase in the size of the faults with increase of the maximum load, result in increased susceptibility to crack initiation. The independence of the lateral crack initiation loads with the total contact time and maximum load may be due to their being less susceptibility of the lateral crack nuclei to stress corrosion because of their more sub-surface location. The median-radial crack morphology beneath 1 and 4 kgf indentation sites was essentially half-penny, with lateral cracks initiating near the base of the damage zone.

Acknowledgements The authors would like to thank the National Science Foundation (NSF) Industry-University Center for Glass Research (CGR) at Alfred University for financial support of this work.

References

1. Frolich F, Grau P, Grellmann W (1977) Phys Stat Sol (a) 42:79
2. Loubet JL, Georges JM, Meille G (1986) In: Blau PJ, Lawn BR (eds) Microindentation techniques in materials science and engineering, ASTM STP 889. American Society for Testing and Materials, Philadelphia, PA, pp 72–89

3. Weiss HJ (1987) Phys Stat Sol (a) 99:491
4. Cook RF, Pharr GM (1990) J Am Ceram Soc 73(4):787
5. Frischat GH (1985) In: Kurkjian CR (ed) Strength of inorganic glass. Plenum Press, New York, pp 135–145
6. Pharr GM, Cook RF (1990) J Mater Res 5(4):847
7. Wagner CJ (1998) Influence of composition on crack initiation behavior of glasses. M.S. Thesis. Alfred University, Alfred, NY
8. Lawn BR, Dabbs TP, Fairbanks CJ (1983) J Mater Sci 18(9):2785
9. Canfield NL (2000) Effects of alkali and alkaline earth additions on the mechanical properties of silicate glasses. M.S. Thesis. Alfred University, Alfred, NY
10. Doerner MF, Nix WD (1986) J Mater Res 1(4):601
11. Anstis GR, Chantikul P, Lawn BR, Marshall DB (1981) J Am Ceram Soc 64(9):533
12. Arora A, Marshall DB, Lawn BR (1979) J Non-Cryst Sol 31(3):425
13. Hagan JT, Van der Zwaag S (1984) J Non-Cryst Sol 64(1–2):249
14. Dabbs TP, Fairbanks CJ, Lawn BR (1984) In: Freiman SW, Hudson CM (eds) Methods for assessing the structural reliability of brittle materials, ASTM STP 844. American Society for Testing and Materials, Philadelphia, PA, pp 142–153
15. Hagan JT (1980) J Mater Sci 15(6):1417